International Geology Review, Vol. 45, 2003, p. 753–766.

Chemostratigraphic Correlation of Upper Permian Lavas from Yunnan Province, China: Extent of the Emeishan Large Igneous Province

LONG XIAO,[1] YI-GANG XU,

Guangzhou Institute of Geochemistry, Chinese Academy of Sciences, Guangzhou 510640, People's Republic of China

SUN-LIN CHUNG,

Department of Geosciences, National Taiwan University, Taipei, Taiwan

BIN HE, AND HOUJUN MEI

Guangzhou Institute of Geochemistry, Chinese Academy of Sciences, Guangzhou 510640, People's Republic of China

Abstract

Although the mantle plume model has been increasingly adopted for generation of the Emeishan basalts, doubts have been cast on the viability of this model because of the relatively small dimensions of this large igneous province (LIP) compared with typical LIPs. The Emeishan LIP was traditionally thought to be bounded on the southwest by the Ailaoshan-Red River (ASRR) fault zone. However, pre-Cretaceous strata in the Jinping area, southwest of the ASRR fault zone, are comparable to those at Binchuan in the western margin of the Emeishan LIP. This correlation is reinforced by similar chemostratigraphic variation of Upper Permian basalts from these spatially separated regions. Therefore, the Jinping basalts, which crop out ~500 km southeast of the Binchuan counterpart, are interpreted as a dismembered part of the Emeishan basalts that were displaced to the present location by mid-Tertiary sinistral movement along the ASRR fault. We suggest that the ASRR fault does not bound the Emeishan LIP. Thus, this LIP has a much larger extent, and its western sector may have extended toward the Paleo-Tethyan ocean, and may have been destroyed by closure in the Triassic.

Introduction

THE EMEISHAN FLOOD BASALTS in southwestern China, one of the oldest Phanerozoic Large Igneous Provinces (LIPs), have recently received much attention, because of the possible connection between flood volcanism and mass extinctions around the Permian–Triassic boundary (e.g., Chung et al., 1998; Wignall, 2001; Lo et al., 2002; Zhou et al., 2002). It has been proposed that the Emeishan basalts were generated by a plume arising from the deep mantle that reached the base of the Yangtze craton during Late Permian time (Chung and Jahn, 1995; Chung et al., 1998; Song et al., 2001; Xu et al., 2001). Although the plume model is consistent with petrologic and geochemical signatures of these basalts (Xu and Chung, 2001; Xu et al., 2001), and is supported by crustal doming immediately preceding eruption (He et al., 2003), doubts have been raised about the viability of this model by some workers in view of the relatively small exposure (~250,000 km^2 in comparison with 1,000,000 km^2 typical of other LIPs; Coffin and Eldholm, 1994) and relatively few volcanic cycles of the Emeishan lavas (e.g., Thompson et al., 2001). The low number of volcanic cycles proposed by Thompson et al. (2001) may be attributable to their observing unrepresentative outcrops. Lava sequences more than 5000 m thick exist in the western Emeishan LIP (i.e., Binchuan; Xu et al., 2001). On the other hand, the Emeishan basalts are remnants of an igneous province that was subjected to intensive destruction and erosion, so the currently accepted surface exposure value of ~250, 000 km^2 is only a minimum estimate.

The Ailao Shan–Red River (ASRR) fault zone is generally considered to represent the western boundary of the Emeishan LIP (Lin, 1985; Zhang et al., 1988). Both petrologic and sedimentary studies, however, suggest that the center of the postulated mantle plume that generated the Emeishan flood basalts was located in western Yunnan Province,

[1]Corresponding author; email: longxiao@gig.ac.cn. Also at State Key Laboratory for Mineral Deposits Research, Department of Earth Sciences, Nanjing University, Nanjing 210093, People's Republic of China.

i.e., in the western part of the Emeishan LIP (Xu et al., 2001; He et al., 2003). The distribution of plume-derived basalts is expected to be symmetric around the locus of the plume (e.g., Campbell and Griffiths, 1990). The asymmetric distribution of the Emeishan basalts (Fig. 1) implies that its western sector may have been cut off during post-eruptional tectonic movements (Chung et al., 1998). It is possible that Upper Permian basalts and mafic complexes exposed at Jinping (southwestern Yunnan province) and in northern Vietnam (Glotov and Polyakov, 2001) constitute a westerly extension of the Emeishan LIP. Disruption of these members from the former Emeishan LIP may be related to mid-Tertiary continental extrusion of Indochina relative to South China along the ASRR fault zone (Tapponnier et al., 1990; Wu, 1993; Chung et al., 1997).

This idea can be tested via stratigraphic comparison of lava successions occurring on either side of the ASRR fault zone. For this purpose, a series of stratigraphic horizons for volcanic successions at Binchuan and Jinping in Yunnan Province (Fig. 1) have been sampled. These localities were chosen because both lava sections are thick (> 4000 m), and more importantly, previous studies revealed a considerable compositional diversity at Binchuan (Xu et al., 2001). Hence, this would ensure the suitability of applying the chemostratigraphic approach to relate two spatially separated distal sections. This paper presents new geochemical and chemostratigraphic data from these rocks. It will be shown that the Jinping basalts are well correlated with those at Binchuan in terms of rock types and stratigraphic variation. Although located outside of the Emeishan LIP, the Jinping basalts are an intrinsic member of the Emeishan basalts. The identification of Emeishan basalts to the west of the ASRR fault zone implies a significantly larger field for the former Emeishan LIP. The fate of this west sector was closely linked with the evolution of the Paleo-Tethyan ocean, which separated the Yangtze craton from the Indochina block.

Geological Setting and Stratigraphic Sequences at Jinping and Binchuan

The Emeishan LIP is located in Yunnan, Sichuan, and Guizhou provinces, southwestern China. The thickest volcanic succession crops out at Binchuan, western Yunnan Province (Fig. 1); it consists of a range of rock types, including low-Ti and high-Ti basalts, picrites, and rhyolites (Huang et al., 1988; Xu et al., 2001). The Upper Permian basalts also occur west of the ASRR fault zone, particularly at Jinping, southwestern Yunnan Province (Fig. 1), located about 500 km southeast of the Binchuan area. The Jinping basalts cover an area of more than 400 km^2, with a lava thickness of up to 4536 m (Yunnan, 1990). However, petrological and geochemical investigations have not yet been carried out on this massive basaltic province, except for a few analyses reported by Chung et al. (1997). As at Binchuan, the Jinping basalts unconformably overlie the upper Middle Permian Maokou Formation, and are in turn overlain by Lower Triassic sedimentary clastic rocks.

Further insight into the geological features at Binchuan and Jinping can be gained from Figure 2, which summarizes the Pre-Cambrian to Quaternary stratigraphic sequences at the two localities. The strata at Pingbian are also included in Figure 2 because this locality is spatially close to Jinping but is situated east of the ASRR fault zone (Fig. 1). It is clear that the pre-Cretaceous stratigraphy of the Jinping area matches that of the Binchuan area very well, despite the large distance between the two localities. Similar observations have been made in earlier studies (Yunnan, 1990; Luo and Zhang, 1992). In contrast, a considerable difference in stratigraphic variation is noted at Jinping and Pingbian, although these locations are close to one another. Specifically, the most prominent difference is the absence of Upper Permian basalts at Pinbian. These stratigraphic relationships suggest that the Jinping area was spatially connected with the Binchuan area during most of its geological history. At Jinping and Binchuan, the Paleogene and younger strata are different, indicating that their separation took place some time between Late Cretaceous and Paleogene time. This separation is most likely related to Cenozoic sinistral movement of the Indochina block along the ASRR fault zone (Tapponnier et al., 1990; Chung et al., 1997). The good correlation of Pre-Cretaceous strata at Binchuan and Jinping provides evidence for a possible genetic link between the Jinping basalts and the Emeishan basalts. A more rigorous assessment of their relationship can be made through direct comparison of the two lava successions themselves, in terms of petrological and geochemical criteria.

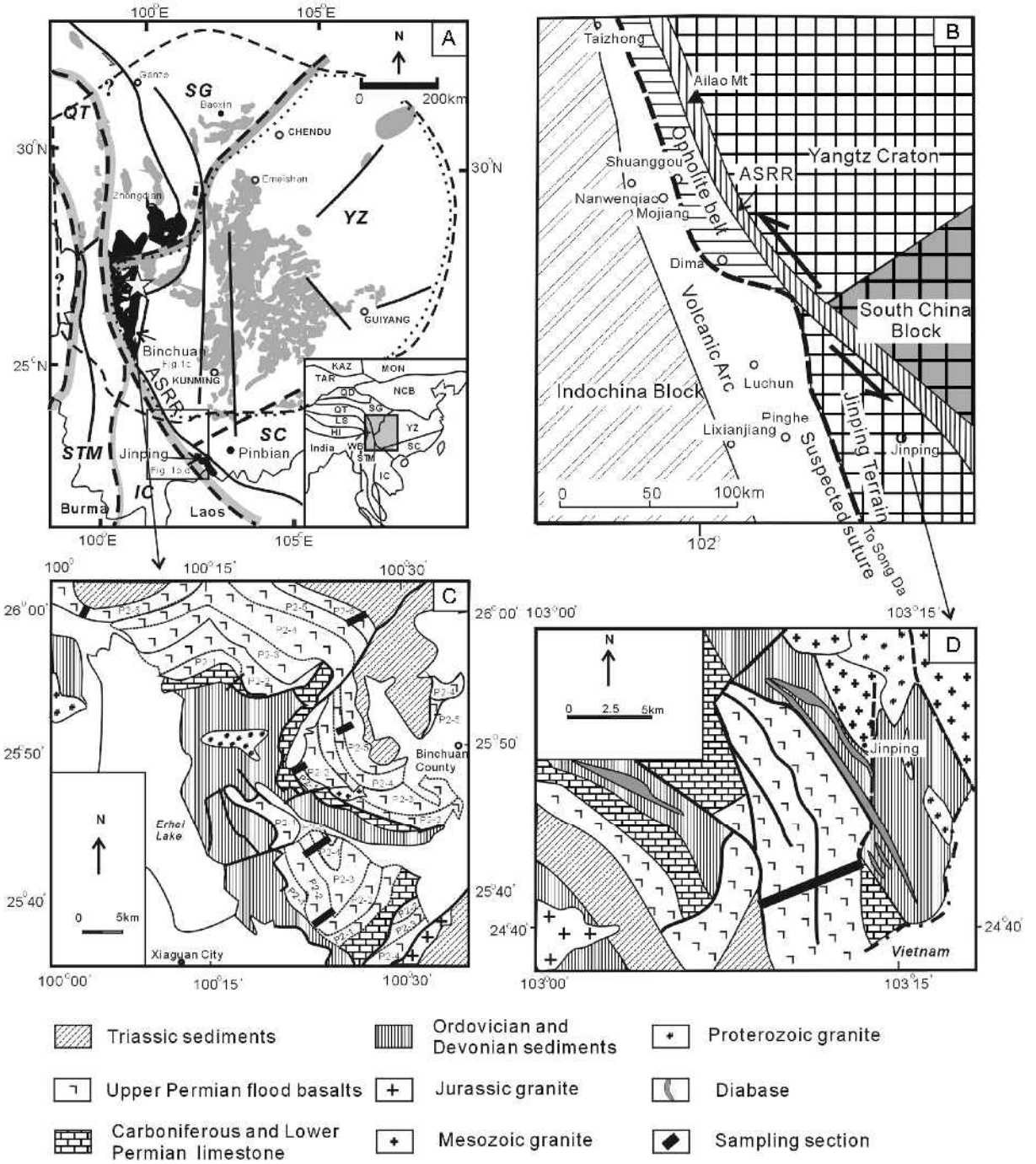

FIG. 1. A. Schematic map showing the distribution of the Late Permian volcanic successions (grey and black areas show HT basalts and LT + HT basalts, respectively) in the Emeishan LIP (modified after Xu et al., 2001). B. Tectonic framework in Jinping area (modified after Luo and Zhang, 1992; Mo et al., 1998; Zhong, 1998). Local geology and sampling locations are shown in (C) for Binchuan and (D) for Jinping, respectively. Major terranes: SC = South China block; YZ = Yangtze craton; SG = Songpan-Ganze accretionary complex; QT = Qiangtang; STM = San-Thai-Malay; IC = Indochina; WB = West Burma; HI = Himalayan; LS = Lhasa; QD = Qaidam; TAR = Tarim; KAZ = Kazkhstan; MON = Mongolia; NCB = North China block). P2-1, P2-2, P2-3, P2-4, P2-5, and P2-6 in Figure 1C are subunits of the Emeishan flood basalts. The star shows the postulated center of the Emeishan mantle plume impact. Arrows indicate the sampling localities. The fine dotted line and dashed line illustrate the previously defined (Lin et al., 1986; Huang et al., 1988) and currently postulated areas of the Emeishan LIP, respectively. The Jinping terrain was initially located near the Dali (Binchuan) area. It was dismembered by sinistral movement along the marginal Ailao Shan–Red River fault zone during Cenozoic time.

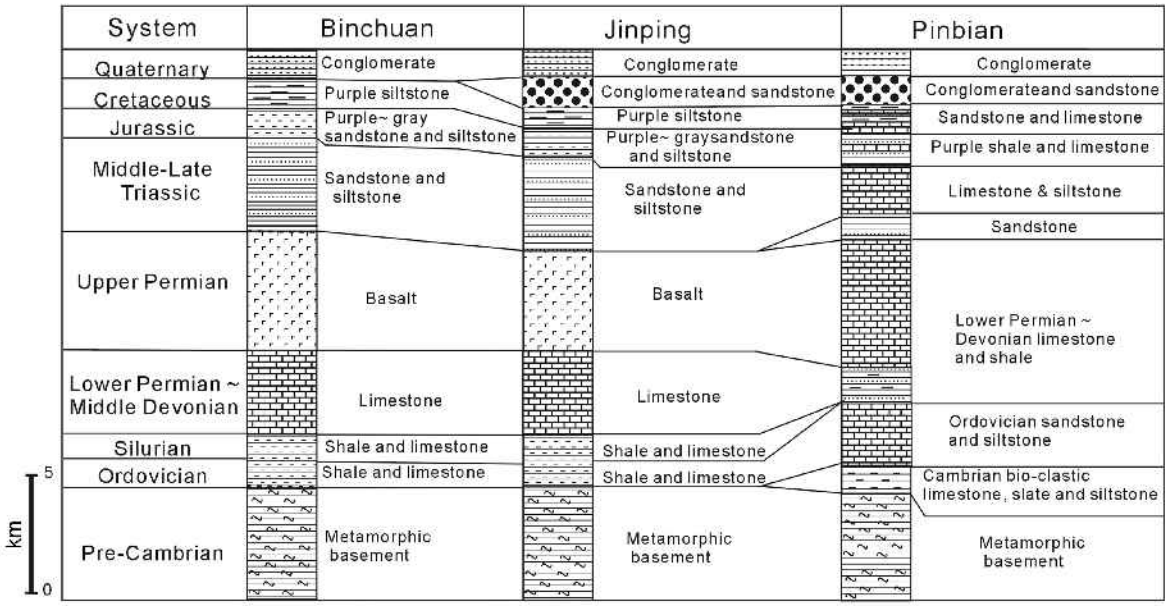

FIG. 2. Comparison of stratigraphy at the Binchuan, Jinping, and Pinbian areas.

Chemostratigraphic Comparison of Permian Basalts at Jinping and Binchuan

As the thickest lava succession in the Emeishan LIP, the Binchuan section serves as a reference for comparison with other basalt members. We will first deal with the rock classification of the Binchuan section and the petrographic and geochemical description of the different rock types. Secondly, the same classification scheme will be applied at Jinping to unravel the petrologic and compositional diversity of the basalts from this locality. Finally, the different rock types, especially their stratigraphic variations, will be compared in the two sections.

The Binchuan basalts

Classification and geochemical characteristics. The measured Binchuan section exceeds 5000 m, and comprises dominantly basaltic lava flows with subordinate trachytic and rhyolitic rocks in the uppermost sequence (Fig. 3). Sixty basaltic samples were collected from this section and were analyzed for major and trace elements, using ICP-AES and ICP-MS, respectively. All the measurements were carried out in the Guangzhou Institute of Geochemistry, Chinese Academy of Sciences. Analytical uncertainties are 1–2% for major elements, 5% for rare-earth elements, and 5–10% for trace elements. Details of the analytical procedures are given in Liu et al. (1996) and Xu (2002). Representative analyses are listed in Table 1.

Two rock types, namely high-Ti and low-Ti basalts, have been classified for the Emeishan basalts on the basis of a small number of analyses for the samples from Binchuan and Ertan (Xu et al., 2001). The high-Ti group (HT) generally has higher Ti/Y (>500) and TiO_2 (>3.7 wt%) than the low-Ti group (LT) (Ti/Y <500, TiO_2 <2.5 wt%). This classification scheme is confirmed by the large database for the Binchuan basalts obtained in this study (Fig. 4). Moreover, available data permit a further subdivision of the low-Ti group into LT1 and LT2 types on the basis of trace element characteristics.

In general, the LT1 basalts have higher Mg# (0.67–0.61) than the LT2 basalts (Mg# = 0.54–0.48) (Table 1). A more evolved nature characterizes the HT basalts, for which Mg# varies between 0.53 and 0.44 (Fig. 4A). Distinction between the LT1 and LT2 lavas is also clear in the plot of Th/Nb and Sm/Yb versus Ti/Y, which highlights the high contents of highly incompatible elements in the LT1 lavas (Figs. 4B and 4C). LT1 lavas have Sm/Yb (3>Sm/Yb>2) ratios higher than LT2 (<2) and lower than the HT lavas (>3), and higher Th/Nb (>0.17) ratios than the LT2 and HT basalts (Th/Nb <0.17).

Differences between these three groups are also easily recognized in a comparison of their REE patterns and multiple-element spidergrams (Fig. 5). Among the three groups, the HT magmas show the highest LREE concentrations, with $(La/Yb)_N$ ranging from 14 to 17 (Table 1; Fig. 5A). In the primitive

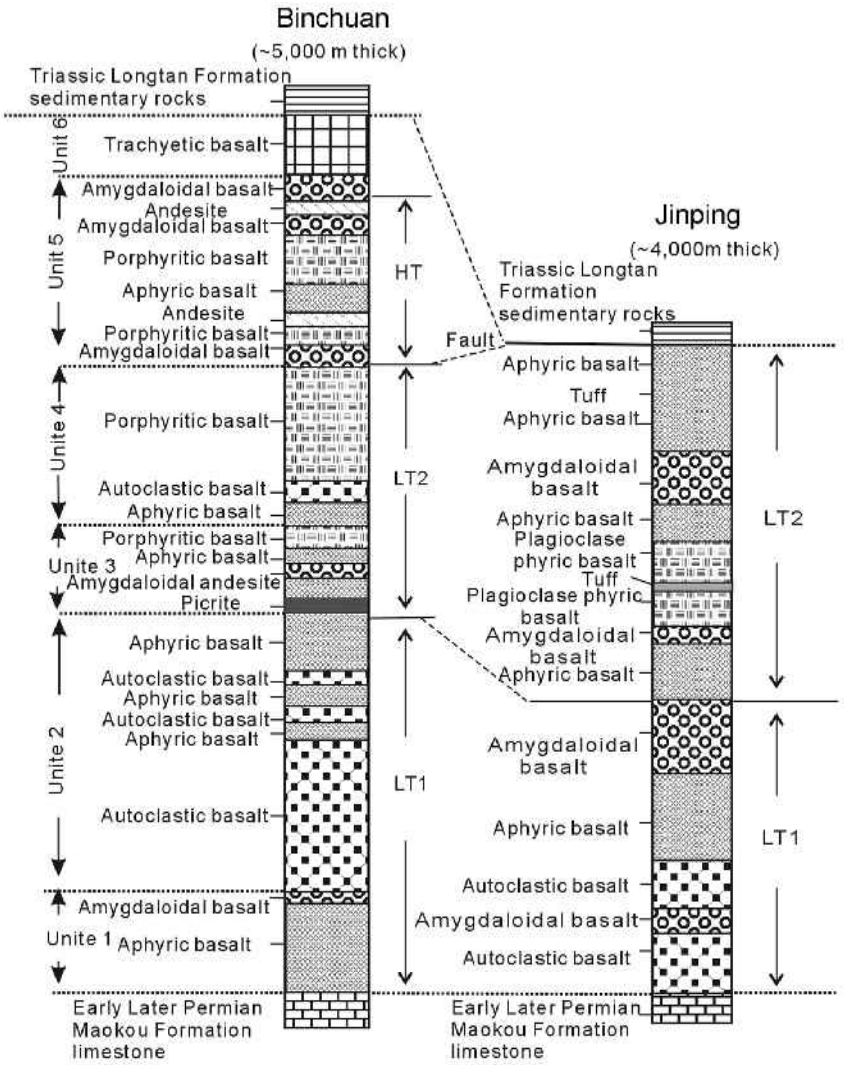

FIG. 3. Composite stratigraphy of Upper Permian basalts from Binchuan and Jinping.

mantle– normalized spidergrams, the HT lavas are characterized by depletion of Rb and Ba relative to Th, and by marked negative Sr anomalies (Fig. 5B). No significant negative Nb anomaly is noted in the samples of this group. Much lower contents of LREE are observed in the low-Ti lavas. Specifically, the LT2 basalts show lower LREE contents [$(La/Yb)_N$ = 2–4.8] than the LT1 basalts [$(La/Yb)_N$ = ~5–8] (Table 1). Weak negative Eu anomalies are noted in the LT1 lavas, but are not observed in the LT2 samples (Fig. 5C). Significant differences between the LT1 and LT2 basalts is also evident in the spider diagrams (Figs. 5D–5F). The LT1 basalts show pronounced negative Nb and Ta anomalies. In contrast, no anomalies for Nb and Ta are associated with the LT2 basalts. Although variable, positive Sr anomalies are present in some LT2 lavas, in contrast to the weak negative Sr anomalies in the LT1 samples.

Petrography. The rock types classified on the basis of compositional criteria show distinct petrographic features in terms of phenocryst and groundmass compositions. The LT1 lavas are mainly aphyric and subordinately phyric. Phenocrysts in phyric rocks are plagioclase (5–10%), olivine (2–8%), and clinopyroxene (2–6%). The groundmass is comprised of plagioclase (25–60 %), basaltic glass (20–45%), and minor magnetite (3–5%). The LT2 type is characterized by clinopyroxene and plagioclace phenocryst-dominated phyric basalts, which are locally interbedded with aphyric basalts. Phenocrysts in the phyric rocks are plagioclase (2–6%) and clinopyroxene (1–7%). The mineral assemblage in the groundmass is similar to that of the LT1 basalts. The HT basalts are phyric, with plagioclase as the dominant phenocryst (10–20%). Clinopyroxene phenocrysts are minor (1–2%).

TABLE 1. Representative Major Oxides and Trace-Element Abundances of Late Permian Basalts from the Jinping and Binchuan Areas

	Jinping													
	LT1					LT2								
Sample	jp-17	jp-18	jp-19	jp-20	jp-21	jp-3	jp-4	jp-7	jp-8	jp-9	jp-11	jp-12	jp-13	jp-15
							wt%							
SiO_2	55.98	53.28	53.82	55.89	50.81	49.25	47.33	47.71	47.68	47.56	48.54	50.40	48.41	55.49
TiO_2	1.53	1.39	1.37	1.87	1.92	2.29	2.34	2.09	2.15	1.96	2.28	2.14	1.49	1.61
Al_2O_3	14.39	15.04	14.71	11.67	12.90	13.10	13.49	14.42	13.57	12.60	12.38	14.58	13.90	14.23
Fe_2O_3	1.53	1.36	1.52	1.54	1.63	2.29	2.38	2.29	2.32	2.19	2.47	2.14	1.67	1.56
FeO	7.83	6.94	7.76	7.84	8.30	11.67	12.13	11.67	11.81	11.18	12.59	10.89	8.52	7.96
MnO	0.15	0.13	0.15	0.15	0.15	0.25	0.24	0.24	0.27	0.24	0.32	0.38	0.14	0.14
MgO	5.66	5.72	6.95	5.27	7.92	6.27	6.27	4.99	7.61	6.29	5.55	6.11	7.48	5.30
CaO	5.05	8.74	8.58	8.56	10.63	6.33	5.96	9.11	6.90	10.15	9.26	4.40	11.97	5.50
Na_2O	2.47	2.42	2.00	3.17	1.88	3.76	5.03	4.46	3.66	3.43	3.19	2.95	2.51	2.33
K_2O	2.85	1.53	1.43	0.71	0.41	1.84	0.35	0.06	0.28	0.06	1.25	1.14	1.31	2.03
P_2O_5	0.21	0.13	0.18	0.16	0.17	0.20	0.25	0.23	0.19	0.22	0.22	0.10	0.22	0.20
LOI	3.31	3.82	2.30	2.65	3.90	2.87	3.72	3.63	3.63	3.68	1.08	4.00	2.38	2.96
Total	100.97	100.52	100.80	99.50	100.66	100.14	99.53	100.92	100.12	99.61	99.14	99.27	100.03	99.34
Mg#[1]	0.51	0.57	0.60	0.49	0.62	0.41	0.40	0.35	0.47	0.43	0.35	0.43	0.60	0.48
							ppm							
Ba	689.70	298.70	358.80	112.20	75.90	731.60	105.50	11.90	45.90	17.80	444.40	371.90	466.30	467.00
Rb	105.40	40.88	71.39	16.50	10.38	48.24	3.89	0.55	6.87	0.99	34.27	32.41	29.59	29.41
Sr	425.80	149.30	416.20	128.70	100.60	284.80	100.40	82.60	426.40	67.20	389.40	318.20	337.90	340.00
Y	31.17	28.30	32.46	28.34	29.26	35.62	36.49	29.11	30.92	34.54	36.55	33.57	23.05	23.09
Zr	190.40	183.90	187.60	179.90	114.00	153.30	158.60	134.20	135.50	133.00	142.20	214.30	124.90	125.80
Nb	16.98	14.53	13.96	17.39	16.80	15.92	15.99	14.28	14.70	14.26	15.72	26.43	14.38	14.34
Th	7.48	7.11	6.75	4.65	4.26	1.70	1.74	2.30	1.51	1.64	1.60	4.04	1.66	1.63
Ga	18.31	22.42	21.58	17.43	22.59	20.88	21.61	33.78	19.11	21.97	21.17	22.51	19.18	19.07
Ni	4.55	39.08	63.57	81.40	83.64	83.28	52.54	79.70	67.09	99.55	50.39	66.50	116.50	116.50
V	241.0	215.7	231.4	252.0	275.2	416.0	361.2	357.4	411.2	399.9	472.5	263.4	258.7	259.8
Cr	127.5	270.2	332.2	194.1	323.9	46.3	52.6	48.9	38.9	44.3	24.1	72.5	325.3	327.2
Hf	4.65	4.35	4.36	4.20	3.29	3.89	3.78	3.17	3.26	3.23	3.58	4.76	3.06	2.95
Cs	2.37	0.54	0.92	0.69	0.66	0.80	0.21	0.13	0.90	0.22	0.38	1.30	0.64	0.65
Sc	29.60	27.61	29.12	27.32	30.94	39.18	38.56	25.79	40.36	42.24	39.56	32.96	30.49	30.26
Ta	1.07	0.90	0.88	1.08	1.06	0.96	0.91	0.85	0.87	0.84	0.93	1.49	0.81	0.81
Co	31.62	31.93	39.69	39.11	43.85	48.60	52.10	42.49	52.25	53.39	54.49	48.98	46.46	46.44
U	1.52	1.56	1.49	1.11	0.73	0.41	0.36	0.45	0.29	0.35	0.37	0.68	0.42	0.40
La	27.19	25.49	25.09	20.47	22.08	12.29	10.74	15.17	9.91	12.69	10.43	19.35	11.00	10.89
Ce	54.25	50.06	50.04	42.65	45.75	26.59	25.92	30.16	23.08	27.13	24.30	41.00	23.90	23.71
Pr	7.04	6.32	6.45	5.82	6.13	3.85	3.91	4.54	3.33	3.85	3.62	5.58	3.37	3.35
Nd	28.70	25.02	26.49	24.20	26.49	18.14	18.51	20.17	15.20	17.36	17.22	23.54	15.38	15.01
Sm	6.03	5.25	5.73	5.34	5.88	4.80	5.07	4.75	4.05	4.50	4.78	5.39	3.83	3.79
Eu	1.57	1.45	1.51	1.59	1.85	1.73	1.71	1.63	1.47	1.56	1.75	1.64	1.38	1.35
Gd	6.39	5.52	5.86	5.46	6.06	6.00	6.00	5.36	4.97	5.57	6.01	6.00	4.46	4.35
Tb	0.98	0.86	0.98	0.89	0.94	1.02	1.01	0.87	0.86	0.93	1.02	1.00	0.71	0.69
Dy	5.55	4.89	5.56	4.98	5.22	6.14	6.13	4.91	5.17	5.64	6.18	5.91	4.11	4.02
Ho	1.05	0.92	1.04	0.92	0.94	1.19	1.21	0.93	1.03	1.13	1.23	1.15	0.79	0.77
Er	2.86	2.48	2.95	2.49	2.56	3.28	3.26	2.60	2.78	3.07	3.38	3.12	2.10	2.08
Tm	0.42	0.37	0.42	0.36	0.36	0.50	0.48	0.36	0.42	0.45	0.51	0.46	0.32	0.31
Yb	2.64	2.32	2.71	2.20	2.23	3.12	2.96	2.28	2.65	2.87	3.24	2.91	1.96	1.96
Lu	0.42	0.38	0.41	0.35	0.35	0.50	0.46	0.35	0.43	0.46	0.51	0.46	0.31	0.30
Ti/Y	335	332	395	438	459	422	404	480	443	379	414	419	444	445
REE	145.0	131.3	135.2	117.7	126.8	89.1	87.3	94.0	75.3	87.2	84.1	117.5	73.6	72.6
Th/Nb	0.44	0.49	0.48	0.27	0.25	0.11	0.11	0.16	0.10	0.12	0.10	0.15	0.12	0.11
(La/Yb)n	7.4	7.88	6.65	6.67	7.12	2.82	2.60	2.74	2.19	3.17	2.31	4.78	4.63	3.98
Sm/Yb	0.36	0.36	0.41	0.31	0.35	0.30	0.32	0.33	0.28	0.32	0.30	0.20	0.27	0.26
Nb/U	11	9	9	15	23	39	44	31	50	41	42	38	34	35
Zr/Nb	11.2	12.6	13.4	10.3	6.7	9.6	9.9	9.4	9.2	9.3	9.0	8.1	8.6	8.7
La/Nb	1.60	1.75	1.80	1.18	1.31	0.77	0.67	1.06	0.67	0.89	0.66	0.73	0.76	0.76
Ba/Nb	40.62	20.56	25.70	6.45	4.52	45.95	6.60	0.83	3.12	1.25	28.27	14.07	32.43	32.57

(*Table continues*)

TABLE 1. *Continued*

	Binchuan														
	LT1							LT2						HT	
Sample	sc-2	sc-3	wl-6	wl-10	wl-12	wl-14	wl-22	wl-25	wl-26	wl-28	wl-29	wl-33	ry-2	ry-5	ry-8
								wt%							
SiO_2	49.91	51.44	52.10	47.46	47.70	49.84	51.61	48.26	46.41	50.46	46.08	52.60	48.11	48.34	45.68
TiO_2	1.59	1.38	1.31	1.42	1.45	1.46	1.70	1.53	1.54	1.65	1.56	1.60	4.48	4.34	4.50
Al_2O_3	13.65	14.37	12.88	12.61	12.60	14.25	12.38	14.80	14.03	14.54	14.39	13.39	13.46	13.25	14.93
Fe_2O_3	1.68	1.50	1.47	1.57	1.63	1.54	2.04	2.01	1.92	1.87	1.83	1.82	2.18	2.15	2.13
FeO	8.57	7.67	7.52	8.88	8.31	7.86	10.39	10.26	10.12	9.54	9.33	9.30	11.11	10.95	10.88
MnO	0.16	0.14	0.13	0.15	0.15	0.14	0.18	0.21	0.18	0.17	0.19	0.15	0.19	0.16	0.23
MgO	8.21	6.98	6.40	8.75	9.17	6.93	6.23	5.78	6.68	5.56	4.79	5.06	5.12	4.86	6.88
CaO	10.64	8.73	11.45	11.82	11.24	9.45	8.18	11.04	11.12	5.38	13.18	6.76	8.54	8.06	5.50
Na_2O	2.19	3.85	1.93	1.63	1.94	3.87	4.15	2.94	1.49	4.79	3.09	4.60	3.62	3.45	4.74
K_2O	0.62	0.75	0.37	0.26	0.73	0.33	0.96	1.24	1.35	0.30	0.57	2.45	0.17	2.28	0.33
P_2O_5	0.17	0.16	0.10	0.12	0.13	0.16	0.19	0.18	0.25	0.45	0.43	0.42	0.44	0.42	0.41
LOI	2.09	3.33	4.85	4.83	5.12	3.36	2.89	1.72	4.99	4.39	4.31	1.96	3.02	1.92	3.94
Total	99.50	100.34	100.55	99.51	100.20	99.21	100.93	100.00	99.03	99.16	99.79	100.11	100.47	100.20	100.19
Mg#[1]	0.63	0.62	0.61	0.64	0.67	0.61	0.52	0.50	0.54	0.51	0.48	0.50	0.45	0.44	0.53
								ppm							
Ba	217.50	176.70	85.12	66.80	175.40	83.65	477.80	291.70	246.40	73.54	175.30	646.80	67.85	851.70	122.20
Rb	22.27	18.43	9.37	6.98	17.76	9.20	22.95	33.23	24.27	8.25	16.58	50.84	3.46	69.90	5.64
Sr	464.20	357.40	170.30	132.40	180.40	264.70	379.00	219.30	252.80	540.40	291.40	409.20	892.40	468.60	336.60
Y	25.69	29.28	21.91	23.56	23.38	26.22	30.38	30.83	23.69	24.89	24.37	22.13	46.99	40.60	38.44
Zr	150.60	179.50	108.10	122.90	123.80	141.10	105.30	125.80	106.20	112.90	106.70	103.20	414.80	402.70	415.90
Nb	12.85	12.73	9.76	11.17	11.11	11.21	11.39	11.11	13.70	17.65	16.98	16.45	53.06	51.48	52.62
Th	3.29	6.22	1.86	2.46	2.60	3.58	1.10	2.00	1.41	1.69	1.67	1.40	5.94	6.11	6.21
Ga	19.18	21.38	20.17	20.59	18.05	18.07	14.53	20.81	22.47	19.21	22.50	11.72	22.43	19.54	27.16
Ni	117.6	90.2	120.0	173.5	182.4	34.1	71.7	76.4	79.7	67.4	60.9	57.5	57.0	65.0	78.4
V	290.3	217.5	260.1	289.9	296.0	286.6	368.6	306.6	286.7	323.4	319.5	296.9	388.1	382.7	382.0
Cr	371.70	355.50	265.80	465.90	471.00	141.40	70.91	59.55	61.46	41.03	41.03	27.65	71.58	94.32	104.40
Hf	3.51	4.19	2.54	2.88	2.96	3.36	2.62	2.96	2.51	2.65	2.52	2.62	8.75	8.72	8.99
Cs	2.39	0.07	0.28	0.64	0.61	0.05	0.44	0.36	0.66	0.38	0.96	0.27	0.57	12.11	2.14
Sc	36.57	26.76	27.40	34.26	34.89	33.51	40.51	33.31	26.55	24.24	23.17	22.85	29.92	30.28	31.14
Ta	0.77	0.82	0.58	0.69	0.70	0.71	0.67	0.66	0.72	0.92	0.85	0.90	3.23	3.17	3.25
Co	46.30	38.74	38.80	47.38	49.00	42.85	50.20	47.94	45.62	44.75	41.59	41.31	39.90	36.80	46.58
U	0.74	1.39	0.46	0.59	0.63	0.90	0.24	0.54	0.34	0.41	0.41	0.30	1.45	1.29	0.93
La	15.38	21.01	11.32	12.85	12.62	14.71	8.05	9.69	8.79	10.94	10.81	9.92	47.22	41.14	42.44
Ce	32.80	43.10	23.35	26.73	26.02	31.05	18.52	21.13	19.61	23.65	23.09	21.43	104.20	93.48	91.28
Pr	4.49	5.58	3.30	3.65	3.57	4.33	2.90	3.07	2.81	3.32	3.24	3.04	14.08	12.74	12.03
Nd	19.42	22.70	14.41	15.93	16.02	19.00	13.83	14.45	12.96	15.00	14.63	14.14	57.81	53.45	51.35
Sm	4.55	5.07	3.50	3.89	3.85	4.46	3.82	3.92	3.44	3.70	3.59	3.60	11.48	10.63	10.22
Eu	1.48	1.58	1.25	1.31	1.26	1.33	1.30	1.39	1.22	1.29	1.44	1.23	3.30	3.10	3.18
Gd	4.93	5.26	3.95	4.42	4.44	4.94	4.71	4.95	4.16	4.32	4.23	4.34	10.61	9.56	9.03
Tb	0.77	0.85	0.64	0.70	0.71	0.79	0.83	0.83	0.68	0.71	0.68	0.68	1.57	1.44	1.35
Dy	4.35	4.91	3.65	4.03	4.04	4.51	4.90	5.06	3.99	4.13	3.96	4.00	8.12	7.55	7.18
Ho	0.82	0.95	0.70	0.75	0.76	0.85	0.99	1.01	0.78	0.80	0.78	0.77	1.48	1.35	1.29
Er	2.19	2.58	1.84	2.01	2.14	2.39	2.69	2.87	2.07	2.13	2.08	2.13	3.81	3.47	3.29
Tm	0.31	0.39	0.27	0.29	0.30	0.33	0.40	0.41	0.31	0.32	0.30	0.31	0.53	0.48	0.46
Yb	1.93	2.37	1.63	1.79	1.85	2.10	2.49	2.64	1.87	1.95	1.86	1.93	3.16	2.90	2.78
Lu	0.30	0.38	0.26	0.29	0.28	0.33	0.40	0.41	0.30	0.31	0.30	0.30	0.50	0.46	0.43
Ti/Y	421	281	372	428	395	362	389	314	456	446	446	459	617	703	769
REE	93.7	116.7	70.0	78.6	77.8	91.1	65.8	71.8	63.0	72.5	70.9	67.8	267.8	241.7	236.3
Th/Nb	0.26	0.49	0.19	0.22	0.23	0.32	0.10	0.18	0.10	0.10	0.10	0.09	0.11	0.12	0.12
(La/Yb)n	5.72	6.36	4.97	5.16	5.02	4.88	2.32	2.63	3.37	3.06	4.18	3.68	14.97	16.54	16.26
Sm/Yb	2.36	2.14	2.14	2.18	2.09	2.12	1.54	1.48	1.84	1.89	1.93	1.86	3.64	3.67	3.68
Nb/U	17	9	21	18	17	12	47	20	40	42	41	54	36	39	56
Zr/Nb	11.72	14.10	11.08	11.00	11.14	12.59	9.24	11.32	7.75	6.40	6.28	6.27	7.82	7.82	7.90
La/Nb	1.20	1.65	1.16	1.15	1.14	1.31	0.71	0.87	0.64	0.62	0.64	0.60	0.89	0.80	0.81
Ba/Nb	16.9	13.8	8.7	5.9	15.7	7.4	41.9	26.2	17.9	4.1	10.3	39.3	1.2	16.5	2.3

[1]Mg# = 100Mg/(Mg + Fe).

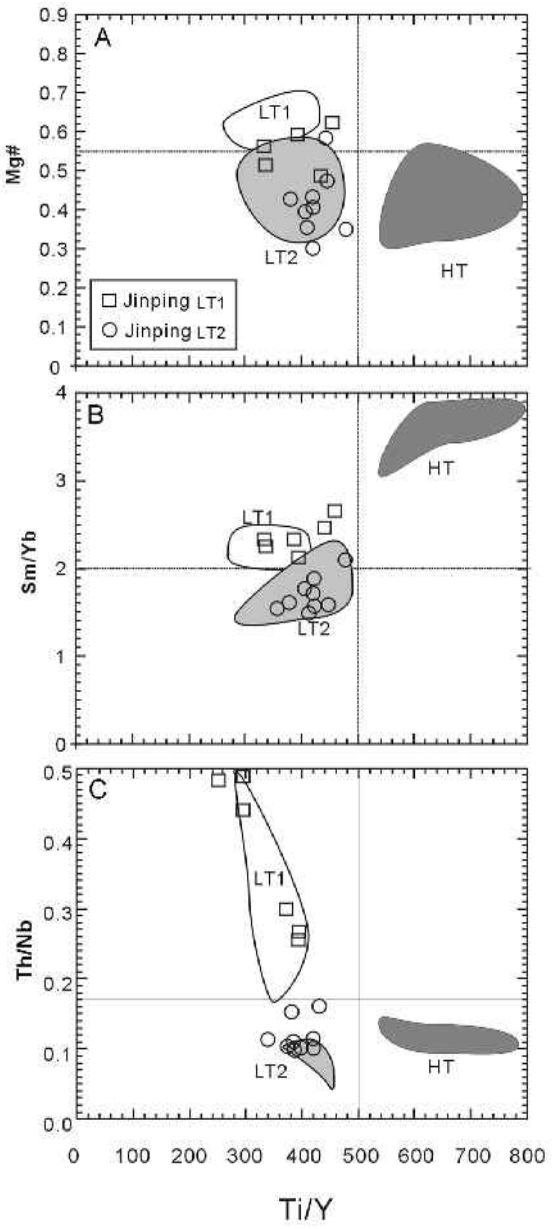

FIG. 4. Plots of Ti/Y versus Mg#, Sm/Yb, and Th/Nb for basalts from the Binchuan and Jinping areas. LT1 and LT2 basalts from Jinping overlap the LT1 and LT2 samples from Binchuan.

The Jinping basalts

When the same classification scheme is applied to the Jinping case, it becomes apparent that the Jinping lava succession consists of LT1 and LT2 basalts (Fig. 3). The Jinping samples are comparable to the respective rock types from Binchuan in terms of major- and trace-element composition (Figs. 4–6). The Jinping LT1 basalts are mainly aphyric, whereas the LT2 samples are mainly phyric. These petrographic features are essentially similar to those for the corresponding types at Binchuan. However, no HT type rocks occur at Jinping.

Chemo-stratigraphic variation

As discussed above, the Jinping basalts display petrographic and geochemical characteristics similar to typical Emeishan basalts of the Binchuan area. This provides the basis for further comparison of stratigraphic variations at the two localities. Mg#, Ti/Y, Th/Nb, and Sm/Yb are suitable criteria for distinguishing the different rock types at Binchuan and Jinping (Fig. 3). Accordingly, these parameters for a given sample are plotted against stratigraphic level in Figure 6. This approach helps to illustrate the changes that occur in volcanic rock types. It is clear from these plots that different rock types occur at certain stratigraphic positions. In the Binchuan case, the LT1 basalts occur at the lowermost part of the lava succession. LT1 basalts are overlain by LT2 lavas, which are in turn are covered by HT basalts. Field observations suggest that the basaltic sequence at Binchuan is capped by silicic magmas of rhyolitic composition. Such a stratigraphic variation is essentially similar to that previously described by Xu et al. (2001).

Only the LT1 and LT2 types are documented in the Jinping area. Nevertheless, available data show that at Jinping, the LT1 basalts are also overlain by LT2 lavas. It can be concluded that the Jinping basalts show the same evolutionary pattern as the Binchuan basalts, although the collected samples from the Jinping section may only correspond to the middle to lower part of the Bingchuan section (Figs. 2 and 3). The absence of HT lavas in the Jinping section may be due to incomplete sampling or, alternatively, may be related to tectonic destruction during sinistral movements (see next section).

Discussion

The Jinping basalts—a dismembered part of the Emeishan LIP

As one of the thickest lava successions, the Binchuan section is representative of the volcanic sequences of the west Emeishan LIP and thus serves as a reference for comparison. Petrologic and geochemical investigations allow classification of the Bingchuan basalts into three rock types, namely LT1, LT2, and HT basalts. These rock types display significantly different petrologic and geochemical

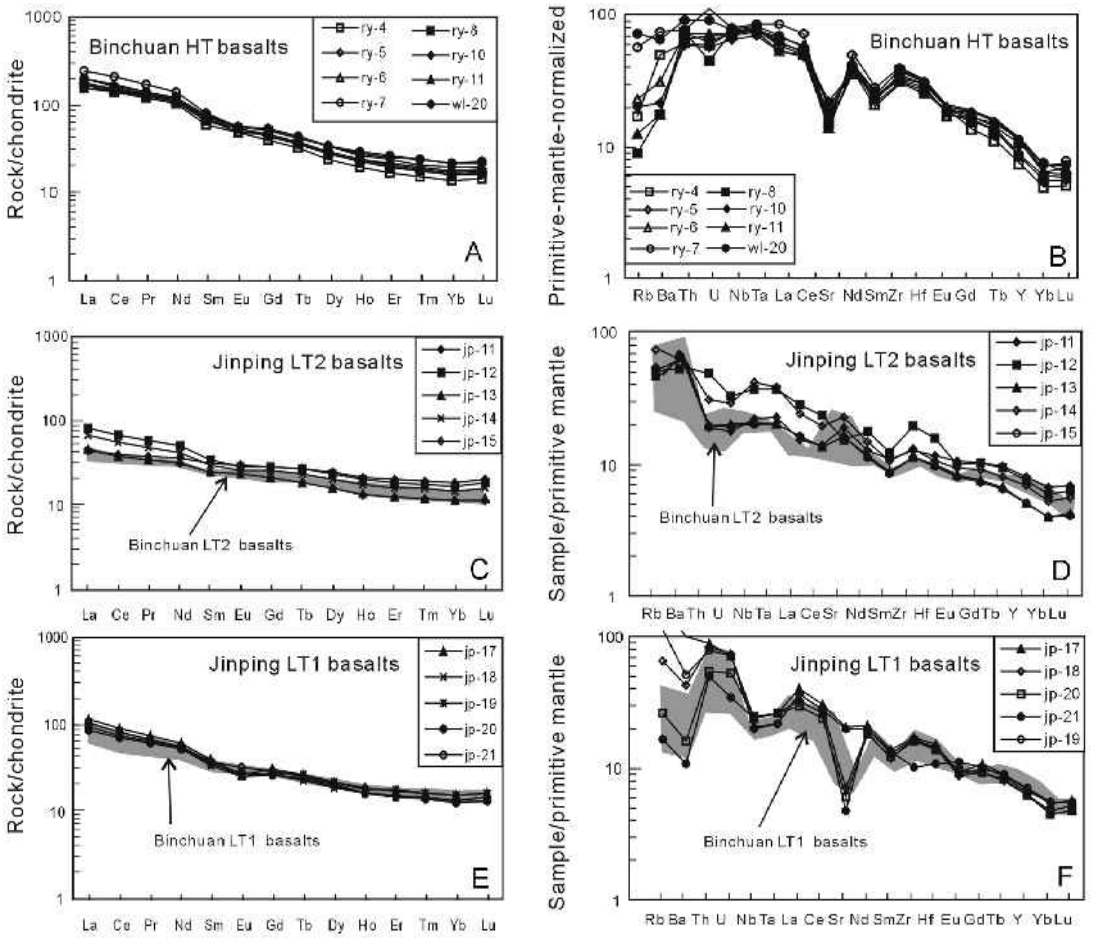

FIG. 5. REE and trace-element abundances in the basalts from Jinping and Binchuan. Normalization values are from Sun and McDonough (1989). For clarity, the compositional ranges of Binchuan LT basalts are shown as shaded areas.

signatures, reflecting different petrogenetic processes. Petrogenetic models for some of these rocks have been discussed by Xu et al. (2001) as part of a reconnaissance study; a more detailed petrogenetic evaluation will be given elsewhere (Xiao et al., 2003). What is emphasized in this study is the stratigraphic relationship between these rocks. As seen in Figures 3 and 5, the LT2 basalts at Binchuan are sandwiched between the LT1 and HT basalts (at the bottom and top, respectively). Thus, in addition to the overall stratigraphic comparison (Fig. 2), the peculiar basaltic rock types and characteristic stratigraphic order between them provide a more precise means of stratigraphic correlation.

The Jinping basalts show similar rock types (except for HT) and, more importantly, the same stratigraphic relationship between the different rock types as seen at Binchuan (Fig. 6). Along with their sedimentary stratigraphic similarities (Fig. 2), these two areas may have been closely associated spatially during a large part of geologic time, but were separated by later tectonic movements. Thus, the Jinping basalts may represent a dismembered part of the Emeishan LIP. Despite the proximal location of Jinping and Pingbian, the strata at the two localities show considerable differences and cannot be correlated over most of the geologic record. Since Jinping and Pingbian are separated by the ASRR fault zone, it is possible that at least one of them is "exotic" and was displaced from other unrelated terrains. The pre-Cretaceous stratigraphic sequences at Jinping, in fact, can be well correlated with those at Binchuan, despite the fact that the two localities are separated by more than 450 km. On a small scale, the Upper Permian basalts in the two localities are also comparable, strongly suggesting that the Jinping terrain may have been originally located near Binchuan. The strata at Binchuan and Jinping differ since Early Paleogene time (Fig. 2). This observation implies that their separation took place at some

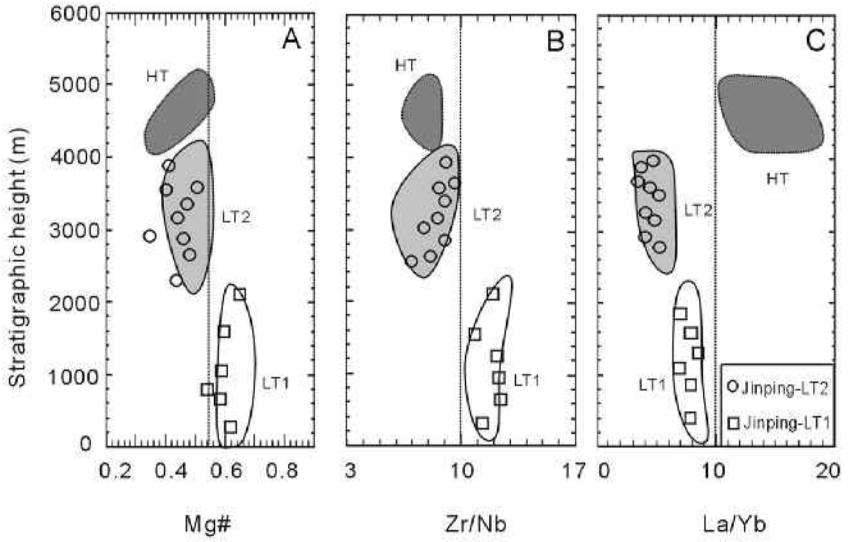

FIG. 6. Variations in selected geochemical parameters with stratigraphic height at Jinping and Binchuan. Shaded areas show the variation ranges of the Binchuan basalts.

time between the Late Cretaceous and Early Paleogene. Therefore, the Cenozoic sinistral movement of the Indochina block along the ASRR fault zone (Tapponnier et al., 1990; Chung et al., 1997) may be the mechanism responsible for the dismemberment of the Emeishan LIP, leading to the occurrence of the Emeishan-type flood basalts in southern Yunnan as well as northern Vietnam.

On the basis of the current distance between Binchuan and Jinping, a minimum of 450 km can be estimated for sinistral displacement along the ASRR fault zone. The actual left-lateral movement could have been greater than 450 km because there was a significant right-lateral movement afterwards (Leloup et al., 1993; Ren and Jin, 1996). In fact, the original position of the Jinping section cannot be precisely constrained because the strata at Lijiang, 150 km north to Binchuan, is also broadly comparable to that at Jinping (Wu, 1993). This represents another source of uncertainty in the displacement estimate.

Constraints on the western boundary of the Emeishan LIP

The close affinity between the Jinping basalts and the Emeishan basalts also has some implications for the western boundary of the Emeishan LIP. Relocation of the Jinping section to the region proximal to Binchuan suggests that the Jinping basalts may represent the western extension of the Emeishan LIP. This suggests that the ASRR fault zone is not the western boundary of the Emeishan basalts, as previously thought (Huang et al., 1988; Zhang et al., 1988). The thickness of the Emeishan basalts varies from over 5000 m in the west (i.e., in western Yunnan Province) to several hundred meters in the east (i.e., in Guizhou Province) over an area 800 km in diameter. If the distribution of the plume-derived basalts is roughly symmetric around the impact site of the plume head, as proposed by Campbell and Griffiths (1990), and the center of the Emeishan plume was located in western Yunnan Province (Xu et al., 2001; He et al., 2003), the remnant Emeishan basalts may only correspond to the core and eastern sector of the original igneous province, and the western sector may have been destroyed during later geologic evolution.

Paleomagnetic studies and plate reconstruction suggest that in the Permian, the western Yangtze craton was a passive continental margin (Huang et al., 1992; Yin and Nie, 1996), and to its west was the paleo-Tethyan ocean (Zhong, 1998). It is therefore highly likely that the basalts in the western sector of the Emeishan LIP were erupted into that oceanic realm. This interpretation is supported by the observation of Upper Permian marine basalts exposed in the Zhongzha terrain and adjacent areas in northern Yunnan Province (Xiao et al., 2003). Preliminary analyses show that these basalts have geochemical features similar to the Emeishan basalts. It is therefore likely that the initial western boundary of the Emeishan LIP occurred somewhere within that ocean (Fig. 7). However, the reconstruction of the Emeishan LIP is difficult to define because closure

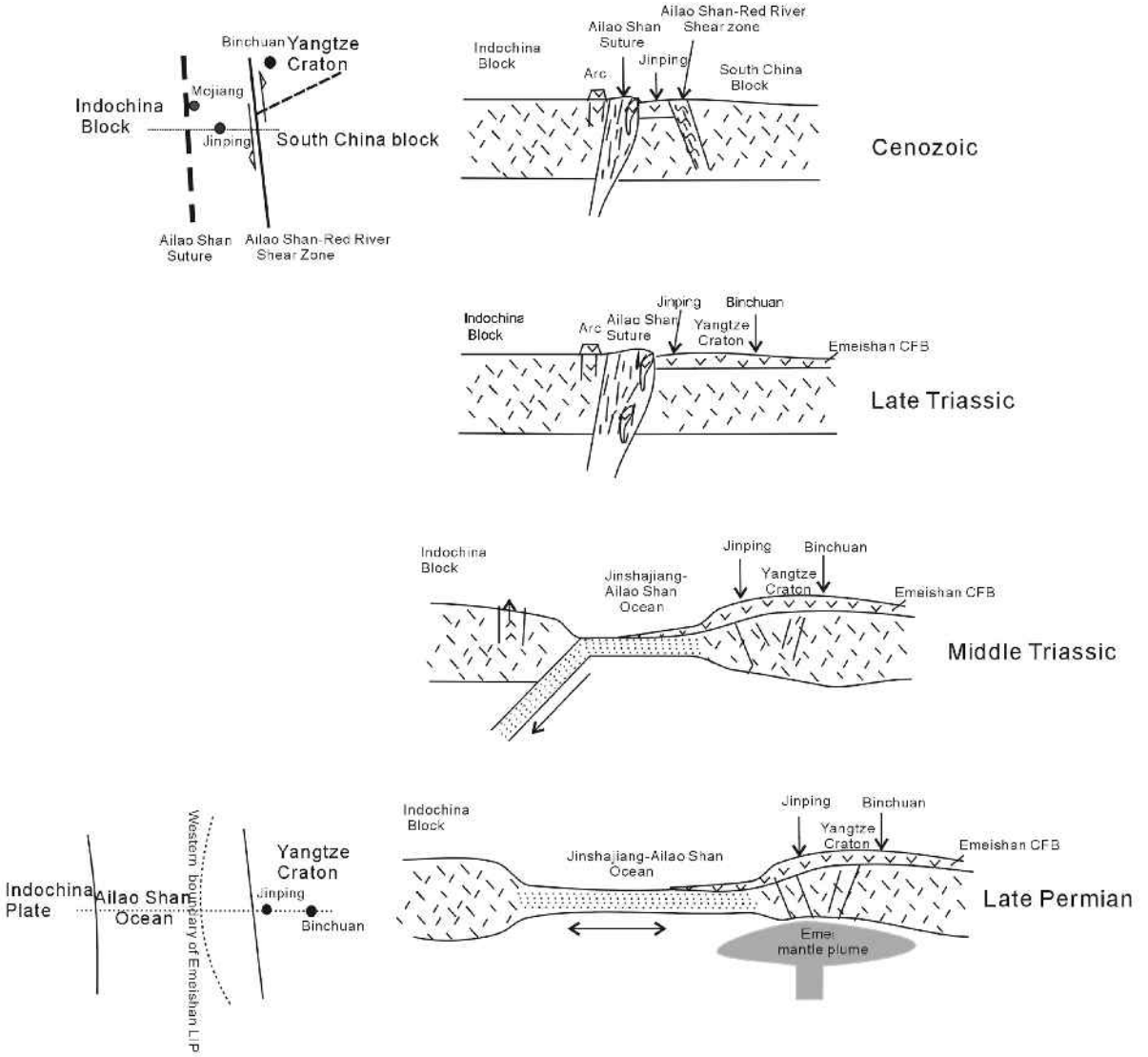

FIG. 7. Schematic diagram illustrating the tectonic evolution of the western margin of the Yangtze craton and the Emeishan LIP from the Late Permian to the Cenozoic.

of the Paleo-Tethyan ocean must have completely dismembered and destroyed the western sector of the former Emeishan province.

Implication for the boundary between the Yangtze and Indochina plates

Many geologists regard the ASRR fault zone as a suture separating the Yangtze craton from the Indochina block (Tapponnier et al., 1986; Leloup et al., 1995; Wang et al., 2000). The main evidence for this interpretation is the occurrence of some dismembered mafic to ultramafic rocks (interpreted as ophiolitic fragments) along the fault zone (Zhang et al., 1994; Wang et al., 2000; Zhang and Zhou, 2000). The identification of Emeishan basalts at Jinping, however, casts considerable doubt on this proposition. Accretion of the Indochina block to the Yangtze craton took place during the Triassic (Yin and Nie, 1986). The close spatial association between the Jinping and Binchuan basalts in the Late Permian (see discussion above) suggests that Jinping belonged to the Yangtze craton, rather than the Indochina block. This is also supported by the similarity of the stratigraphic sequences in the two localities over a prolonged geologic time. The ASRR fault zone is therefore not a suture, but more likely a marginal fault of the Yangtze craton. A similar conclusion was reached by Chung et al. (1997) and Wang et al. (1998), who suggested that the Shuanggou ophiolite could be connected with the Song Da

ophiolite zone in Vietnam. These authors postulated that the actual suture may be along the Mojiang–Lixianjiang–Song Da belt, a few tens of kilometers south of the ASRR fault zone. While concurring with this interpretation, we would also suggest that the suspected suture zone southern Yunnan Province may have been located east of Lixianjiang, somewhere between Luchuan and Jinping (Figs. 1C and 7). Support for this argument comes from the presence of Upper Permian calc-alkaline volcanic-arc rocks at Pinghe, in Luchun County (Wei and Shen, 1997; Mo et al., 1998), which may belong to the volcanic arc belt between the Simao basin and the suspected suture zone.

Conclusions

The pre-Cretaceous strata at Jinping, an area distal from the Emeishan LIP, are comparable with those in the Binchuan area, where typical Emeishan lava successions are preserved. Comparison on a small scale suggests that the Upper Permian basaltic sequences in the two spatially separated regions are correlated in terms of chemostratigraphic variation. Three rock types (namely LT1, LT2 and HT basalts), occur successively from the bottom to the top of the lava section at Binchuan. Although HT basalts are absent, both LT1 and LT2 units are recognized at Jinping, with the LT1 basalts underlying the LT2 lavas. These observations suggest that the Jinping terrain belonged to the Yangtze craton, and the Jinping basalts represent a dismembered part of the Emeishan basalts. Separation of the Jinping basalts from the Emeishan LIP is interpreted as due to Cenozoic sinistral movement of the Indochina block and a part of the western Yangtze craton along the ASRR fault zone (Tapponnier et al., 1990; Harrison et al., 1996; Chung et al., 1997). Identification of the Emeishan basalts to the west of the ASRR fault suggests that the ASRR fault zone does not represent the western boundary of the Emeishan LIP. The asymmetric distribution of the remnant Emeishan basalts around the postulated center of the mantle plume in western Yunnan Province implies that the extent of the Emeishan LIP is much larger than currently believed. The western sector of this LIP may have extended toward the paleo-Tethyan ocean, and may have been destroyed by closure in the Triassic.

Acknowledgments

Dr. Z. Chen is thanked for assistance in the field. We are grateful to Dr. R. Rapp for improving the English exposition. The study was financially supported by the Chinese Ministry of Science and Technology (G1999043205), National Natural Science Foundation of China (40234046), Chinese Academy of Sciences (KZCX2-101), and China Postdoctoral Science Foundation (2002031004). This paper was completed while YGX was a visiting scientist at the National Taiwan University, supported by the National Science Council of Taiwan.

REFERENCES

Campbell, I. H., and Griffiths, R. W., 1990, Implications of mantle plume structure for the evolution of flood basalts: Earth and Planetary Science Letters, v. 99, p. 79–93.

Chung, S. L, and Jahn, B. M., 1995, Plume-lithosphere interaction in generation of the Emeishan flood basalts at the Permian–Triassic boundary: Geology, v. 23, p. 889–892.

Chung, S. L., Jahn, B. M., Wu, G. Y., Lo, C. H., and Cong, B. L., 1998, The Emeishan flood basalt in SW China: A mantle plume initiation model and its connection with continental break-up and mass extinction at the Permian–Triassic boundary, *in* Flower, M. F. J., Chung, S. L., Lo, C. H., and Lee, T. Y., eds., Mantle dynamics and plate interaction in East Asia: American Geophysical Union Geodynamics Series, v. 27, p. 47–58.

Chung, S. L., Lee, T. Y., Lo, C. H., Wang, P. L., Chen, C. Y., Yem, N. G., Hoa, T. T., and Wu, G.. Y., 1997, Intraplate extension prior to continental extrusion along the Ailaoshan–Red River shear zone: Geology, v. 25, p. 311–314.

Coffin, M. F., and Eldholm, O., 1994, Large igneous provinces: Crustal structure, dimensions, and extenal consequences: Reviews of Geophysics, v. 32, p. 1–36.

Glotov, A. I., and Polyakov, G. V., 2001, The Ban Phuc Ni-Cu–PGE deposit related to the Phanerozoic komatiite-basalt association in the Song Da rift, northwestern Vietnam: The Canadian Mineralogist, v. 39, p. 573–589.

Harrison, T. M., Leloup, P. H., Ryerson, F. J., Tapponnier, P., Lacassin, R., and Wenji, C., 1996, Diachronous initiation of transtension along the Ailao Shan-Red River shear zone, Yunnan and Vietnam, *in* Yin, A., and Harrison, T. M., eds., The tectonic evolution of Asia: New York, NY, Cambridge University Press, p. 205–226.

He, B., Xu, Y. G., Chung, S. L., Xiao, L., and Wang, Y., 2003, Sedimentary evidence for a rapid crustal doming prior to the eruption of the Emeishan flood basalts: Earth and Planetary Science Letters, in press.

Huang, K. N., Yang, R. Y., and Wang, X. C., 1988, A preliminary study on trace element geochemistry of Emeishan basalts from SW China: Acta Geological Sinica, v. 4, p. 49–60.

Huang, K. N., Opdyke, N. D., Peng, X. J., and Li, J. G., 1992, Paleomagnetic results from the Upper Permian of the eastern Qiangtang Terrane of Tibet and tectonic implications: Earth and Planetary Science Letters, v. 111, p. 1–10.

Leloup, P. H., and nine others, 1995, The Ailao Shan–Red River shear zone (Yunnan, China): Tertiary transform boundary of Indochina: Tectonophysics, v. 251, p. 3–84.

Leloup, P. H., Harrison, T. M., Ryerson, F. J., Chen, W., Li, Q., Tapponnier, P., and Lacassin, R., 1993, Structural, petrological, and thermal evolution of a Tertiary ductile strike-slip shear zone, Diancang Shan, Yunnan: Journal of Geophysical Research, v. 98, p. 6715–6743.

Lin, J. Y., 1985, Spatial and temporal distribution of Emeishan basaltic rocks in three southwestern provinces (Sichuan, Yunnan, and Guizhou) of China: Chinese Science Bulletin, v. 12, p. 929–932 (in Chinese).

Liu, Y., Liu, H. C., and Li, X. H., 1996, Simultaneous and precise determination of 40 trace elements in rock samples using ICP-MS: Geochemica, v. 25, p. 552–558 (in Chinese).

Lo Chinghua, Chung Sunlin, Lee Tungyi, and Wu Genya, 2002, Age of the Emeishan flood magmatism and relations to Permian–Triassic boundary events: Earth and Planetary Science Letters, v. 198, p. 449–458.

Luo, J. L., and Zhang, Z. G., 1992, Sedimentary geology and mineralization in the Tethys of the Nujiang- Langcangjiang-Jinshajiang area: Beijing, China, Geological Memoirs, MGMR, Geological Publishing House, series 3, no. 17, 231 p. (in Chinese).

Mo, X. X., and eight others, 1998, Volcanics-opholite and mineralization of middle-southern part of the Sanjiang area of southwestern China: Beijing, Geological Publishing House, 128 p. (in Chinese).

Ren, J. S., and Jin, X. C., 1996, New observation of the Red River fault: Geological Review, v. 42, p. 439–442.

Song, X. Y., Zhou, M. F., Hou, Z. Q., Cao, Z. M., Wang, Y. L., and Li, Y. G., 2001, Geochemical constraints on the mantle source of the Upper Permian Emeishan continental flood basalts, southwestern China: International Geology Review, v. 43, p. 213–225.

Sun, S. S., and McDonough, W. F., 1989, Chemical and isotopic systematics of oceanic basalts: Implications for mantle composition and processes, *in* Saunders, A. D., and Norry, M. J., eds., Magmatism in ocean basins: Geological Society of London Special Publication, v. 42, 313–345.

Tapponnier, P., and nine others, 1990, The Ailao Shan–Red River metamorphic belt: Tertiary left-lateral shear between Indochina and South China: Nature, v. 343, p. 431–437.

Tapponnier, P., Peltzer, G., Armijo, R., 1986, On the mechanics of the collision between India and Asia, *in* Coward, M. P., and Ries, A. C., eds., Collision tectonics: Geological Society [London], Special Publication, v. 19, p. 115–157.

Thompson, G.. M., Ali, J. R., Song, X., and Jolley, D. W., 2001, Emeishan basalts, southwest China: Reappraisal of the formation's type area stratigraphy and a discussion of its significance as a LIP: Journal of the Geological Society of London, v. 158, p. 593–599.

Wang, P. L., Lo, C. H., Lee, T. Y., Chung, S. L., Lan, C. Y., and Yem, N. T., 1998, Thermochronological evidence for the movement of the Ailao Shan–Red River shear zone: A perspective from Vietnam: Geology, v. 26, p. 887–890.

Wang, X. F., Metcalfe, I., Jian, P., He, L. Q., and Wang, C. S., 2000, The Jinshajiang–Ailaoshan suture zone, China: Tectonostratigraphy, age, and evolution: Journal of Asian Earth Sciences, v. 18, p. 675–690.

Wei, Q. R., and Shen, S. Y., 1997, Arc volcanic rocks of Late Permian (P2) in Taizhong-Lixianjiang zone, Ailao Shan area: Journal of Mineralogy and Petrology, v. 17, p. 8–16 (in Chinese).

Wignall, P. B., 2001, Large igneous provinces and mass extinctions: Earth Science Reviews, v. 53, p. 1–33.

Wu, G. Y., 1993, Permian basalts in Lijiang and Jinping, western Yunnan: A comparative study and its geological significance: Acta Petrological Sinica (supplement), v. 9, p. 63–69.

Xiao, L., Xu, Y. G., Mei, H. J., and Sha, S. L., 2003, Geochemistry of Emeishan Flood basalts at Binchuan area, SW China: Rock types and temporal evolution: Geological Science, in press (in Chinese).

Xu, Y. G., 2002, Evidence for crustal components in mantle source and constraints on recycling mechanism: Pyroxenite xenoliths from Hannuoba, North China: Chemical Geology, v. 182, p. 301–322.

Xu, Y. G., and Chung, S. L., 2001, The Emeishan large igneous province: Evidence for mantle plume activity and melting conditions: Geochemica, v. 30, p. 1–9.

Xu, Y. G., Chung, S. L., Jahn, B. M., and Wu, G. Y., 2001, Petrologic and geochemical constrints on the petrogenesis of Permian–Triassic Emeishan flood basalts in southwestern China: Lithos, v. 58, p. 145–168.

Yin, A., and Nie, S. Y., 1996, A Phanerozoic palinspastic reconstruction of China and its neighboring regions, *in* Yin, A., and Harrison, M., eds., The tectonic evolution of Asia: Cambridge, UK, Cambridge University Press, p. 442–484.

Yunnan Bureau of Geology and Mineral Resources, 1990, Regional geology of Yunnan Province: Beijing, China, Geological Publishing House, Geological Memoirs, MGMR, series 1, no. 21, 554 p. (in Chinese).

Zhang, Q., Zhou, D. J., Zhao, D. S., Huang, Z. X., Han, S., Jia, Z. Q., and Dong, J. Q., 1994, Ophiolites of the Hengduan Mountains, China: Characteristics and tec-

tonic settings: Journal of Southeast Asian Earth Sciences, v. 9, p. 335–344.

Zhang, Q., and Zhou, G. P., 2000, Opholites of China: Beijing, China, Science Press, 182 p. (in Chinese).

Zhang, Y. X., Lou, Y., and Yang, X., 1988, The Panxi Rift: Geological Press, Beijing, 422 p. (in Chinese).

Zhong, D. L., 1998, The paleo-Tethys orogen in western Yunnan and Sichuan: Beijing, China, Science Press, 231 p. (in Chinese).

Zhou, M. F., Malpas, J., Song X. Y., Robinson, P. T., Sun, M., Kennedy, A. K., Lesher, C. M., and Keays, R. R., 2002, A temporal link between the Emeishan large igneous province (SW China) and the end-Guadalupian mass extinction: Earth and Planetary Science Letters, v. 196, p. 113–122.